Gbx2 is required for the morphogenesis of the mouse inner ear: a downstream candidate of hindbrain signaling

Zhengshi Lin, Raquel Cantos, Maria Patente and Doris K. Wu*

Laboratory of Molecular Biology, National Institutes on Deafness and Other Communication Disorders, National Institutes of Health, Bethesda, MD 20850, USA
*Author for correspondence (e-mail: wud@nidcd.nih.gov)

Accepted 28 February 2005

Development 132, 2309-2318
Published by The Company of Biologists 2005
doi:10.1242/dev.01804

Summary

***Gbx2* is a homeobox-containing transcription factor that is related to *unplugged* in *Drosophila*. In mice, *Gbx2* and *Otx2* negatively regulate each other to establish the mid-hindbrain boundary in the neural tube. Here, we show that *Gbx2* is required for the development of the mouse inner ear. Absence of the endolymphatic duct and swelling of the membranous labyrinth are common features in *Gbx2*$^{-/-}$ inner ears. More severe mutant phenotypes include absence of the anterior and posterior semicircular canals, and a malformed saccule and cochlear duct. However, formation of the lateral semicircular canal and its ampulla is usually unaffected. These inner ear phenotypes are remarkably similar to those reported in *kreisler* mice, which have inner ear defects attributed to defects in the hindbrain. Based on gene expression analyses, we propose that activation of *Gbx2* expression within the inner ear is an important pathway whereby signals from the hindbrain regulate inner ear development. In addition, our results suggest that *Gbx2* normally promotes dorsal fates such as the endolymphatic duct and semicircular canals by positively regulating genes such as *Wnt2b* and *Dlx5*. However, *Gbx2* promotes ventral fates such as the saccule and cochlear duct, possibly by restricting *Otx2* expression.**

Key words: *Gbx2*, *Otx2*, *kreisler*, Hindbrain signaling, Inner ear development, Otic vesicle, Mouse

Introduction

The mammalian inner ear develops from a thickening of the ectoderm adjacent to the hindbrain known as the otic placode, which invaginates to form the otocyst. The teardrop-shaped otocyst then undergoes a series of morphogenetic events to give rise to a structurally complex inner ear, consisting of vestibular and auditory components. In the vestibular component, three semicircular canals and their associated sensory tissues (cristae) housed within the ampullae, are responsible for detecting angular head movements. Two additional sensory tissues, the macula of the utricle and the macula of the saccule, are responsible for sensing gravity and linear acceleration, respectively. The auditory component, the cochlear duct, is a coiled structure in mammals. The molecular mechanisms that govern the development of these various components of the inner ear are largely unknown.

Tissues surrounding the inner ear, such as the hindbrain, mesoderm and endoderm, have been implicated in conferring signals required for inner ear development (for reviews, see Fekete, 1999; Kiernan et al., 2002). The importance of the hindbrain in this process is evident from analyses of mutant mice such as the *Hoxa1* knockout and *kreisler* (for a review, see Kiernan et al., 2002). Both kreisler/*Mafb* and *Hoxa1* are expressed in the hindbrain but not the inner ear, yet inner ears of mice with these genes mutated are abnormal. The inner ear defects of these mutant mice are attributed, in particular, to defects in rhombomere 5 (r5), a region of the hindbrain juxtaposing the developing otic placode (Kiernan et al., 2002). Although the inner ear phenotypes in these mutants are variable, they often include the absence of the endolymphatic duct and an enlargement of the membranous labyrinth. The enlarged membranous labyrinth could be secondary to the loss of the endolymphatic duct, which has been shown to be important in maintaining fluid homeostasis within the membranous labyrinth (Everett et al., 2001; Hulander et al., 2003). In addition to the *kreisler* and *Hoxa1* mutants, knockout of *Raldh2* (retinaldehyde dehydrogenase 2) also results in otocyst malformations that are attributed to a defective hindbrain (Niederreither et al., 2000).

As both kreisler/*Mafb* and *Hoxa1* are transcription factors, their effects on inner ear development are likely to be mediated via the regulation of signaling molecules. Several lines of evidence suggest that FGF3 might be one of these hindbrain-derived signals that mediate inner ear development. First, inner ears of *Fgf3* knockout mice show a similar phenotype to those of *kreisler* and *Hoxa1* mutants (Mansour et al., 1993). Second, FGF3 and kreisler/Mafb are thought to positively regulate each other in the hindbrain (Marin and Charnay, 2000; Theil et al., 2002). Consistent with these results, the expression of *Fgf3* in r5 and r6 is absent in *kreisler* mutants, whereas *Fgf3* expression in the mutant inner ears is present (McKay et al., 1996). Third, knockout of a receptor for FGF3, *Fgfr2(IIIb)*, results in severe inner ear malformations that include an absence of the endolymphatic duct (Pirvola et al., 2000). However, FGF3 may not be the only signaling factor from r5 that mediates inner ear development, as the inner ear phenotypes of *Fgf3* knockout

mice are relatively milder and lower in penetrance when compared with inner ears of *kreisler*, *Hoxa1*, *Raldh2* and *Fgfr2(IIIb)* mutant mice. Furthermore, another *Fgf3* knockout mouse strain that was recently generated has no apparent inner ear phenotype (Alvarez et al., 2003). Therefore, additional signaling factors from the hindbrain including other members of FGF family could be involved in mediating inner ear development. Nevertheless, to date, specific downstream otic genes that are activated by these signaling molecules from the hindbrain remain elusive.

Gbx2 is a homeobox gene that is related to *Drosophila unplugged* (Chiang et al., 1995). The expression of *Gbx2* in the midbrain-hindbrain junction of vertebrates is conserved among several species (Bouillet et al., 1995; Shamim and Mason, 1998; Su and Meng, 2002; von Bubnoff et al., 1996), and knockout of *Gbx2* in mice affects the normal positioning of this junction in the brain (Wassarman et al., 1997). *Gbx2* is also expressed in the otic placode of several species (Bouillet et al., 1995; Shamim and Mason, 1998; Su and Meng, 2002). In mice, the expression of *Gbx2* in the otic placode is correlated with proper otocyst formation, but its specific role in inner ear development is not known (Wright and Mansour, 2003). In this study, we analyzed the inner ears of *Gbx2* knockout mice and show that Gbx2 is a key molecule in patterning both vestibular and auditory components of the inner ear. Based on comparisons of inner ear phenotypes and gene expression analyses between *Gbx2* and some of the hindbrain mutants, in particular, *kreisler*, we postulate that *Gbx2* is an important downstream target of hindbrain signaling.

Materials and methods

Animals

Mice heterozygous for a deletion of the *Gbx2* gene were kindly provided by Alexandra Joyner (New York University). *Gbx2* heterozygous mice were maintained in a Swiss Webster background, and the offspring of these mice were genotyped using PCR as described (Wassarman et al., 1997).

Paint fill and in situ hybridization

Paint-fill analyses and in situ hybridization experiments were performed as described (Morsli et al., 1998). A total of 50 *Gbx2* homozygous mutant embryos between 9.5 and 15.5 dpc were used for in situ hybridization analyses, and a total of 40 $Gbx2^{-/-}$ embryos between 8.5 and 10.5 dpc were processed for whole-mount in situ hybridization. Heterozygous and homozygous *Gbx2* embryos from 8.5 to 9.0 dpc for whole-mount in situ hybridization were age matched based on the total number of somite pairs. RNA probes for bone morphogenetic protein 4 (*Bmp4*), lunatic fringe (*Lfng*), neurofilament protein 68 kDa (*NF68*; Nef1 – Mouse Genome Informatics) and orthodenticle 2 (*Otx2*) were prepared as described (Morsli et al., 1999). RNA probes for *Eya1* (Xu et al., 1997), *Gata3* (Karis et al., 2001), *Gbx2* (Bouillet et al., 1995), *Myo15a* (Anderson et al., 2000), *Neurod1* (Ma et al., 1998) and *Pax2* (Dressler et al., 1990) were prepared according to cited references.

Cell proliferation and apoptosis assays

Cell proliferation and apoptotic assays were performed as described (Burton et al., 2004). Apoptotic cells were identified using terminal dUTP nick-end labeling (TUNEL) method (ApopTag).

Results

Expression of *Gbx2* in the developing inner ear

We first examined the spatial and temporal expression patterns of *Gbx2* in the developing mouse inner ear between 8.5 and 15.5 dpc. *Gbx2* mRNA is first detectable in the otic placode at 8.5 dpc (data not shown) (Wright and Mansour, 2003). In the newly formed otocyst, *Gbx2* transcripts are present in the entire dorsomedial region (Fig. 1A,B; arrow). At 10.5 dpc, the endolymphatic duct forms in the dorsomedial region of the otocyst, and it is *Gbx2* positive (Fig. 1C). In addition, the *Gbx2* expression domain extends ventrally beyond the endolymphatic duct to the equator of the otic vesicle (Fig. 1C,D,F).

We correlated this *Gbx2* expression domain at 10.5 dpc with the location of presumptive sensory patches, using *Bmp4* and *Lfng* as markers. At this age, *Bmp4* is expressed in the three presumptive cristae and *Lfng* is expressed in the other presumptive sensory tissues, the macula utriculi, macula sacculi and organ of Corti, as well as in the neurogenic region that delaminates to form the cochleovestibular ganglion (Morsli et al., 1998). Comparisons of adjacent cryosections probed for *Gbx2* and *Bmp4* transcripts (Fig. 1D,E) or *Gbx2* and *Lfng* transcripts (Fig. 1F,G) show that the *Gbx2* expression domain does not overlap significantly with the presumptive sensory regions. By 13 dpc, only the endolymphatic duct is positive for *Gbx2* hybridization signals, and no *Gbx2* expression within the inner ear is detectable by 15.5 dpc.

In addition, *Gbx2* transcripts are detected in the mid-hindbrain junction at 9.5 dpc (Fig. 1A, arrowheads) (Bouillet et al., 1995), as well as longitudinal columns in the dorsal and intermediate regions of the hindbrain and spinal cord (Fig. 1A,C, asterisks).

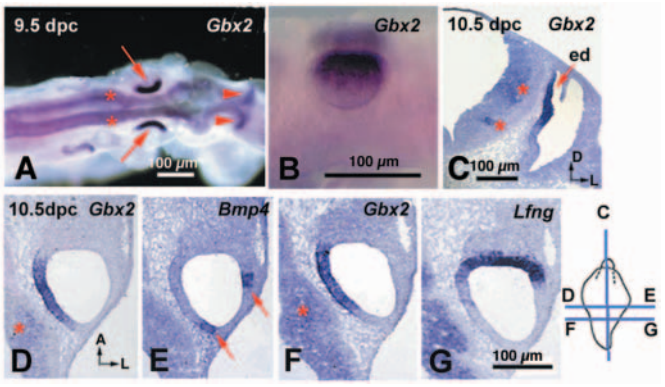

Fig. 1. Expression of *Gbx2* in the developing mouse inner ear. (A) Dorsal view of a mouse embryo at 9.5 dpc probed for *Gbx2* transcripts. Arrows indicate *Gbx2* expression in the otocyst. Arrowheads indicate *Gbx2* expression in the mid-hindbrain junction. (B) An enlarged lateral view of the right otocyst in A, showing *Gbx2* hybridization signals in the dorsomedial half of the otocyst. (C) *Gbx2* expression in the endolymphatic duct (ed) at 10.5 dpc. (D-G) Pairs of 12 μm adjacent sections probed for *Gbx2* (D,F) and *Bmp4* (E) or *Lfng* (G) transcripts. Arrows in E indicate *Bmp4* expression in the presumptive cristae. Asterisks indicate *Gbx2* expression in the neural tube. Approximate levels of sections for C-G are shown in the schematic diagram. Orientation in D applies to D-G; A, anterior; D, dorsal; L, lateral. Scale bar in G applies to D-G.

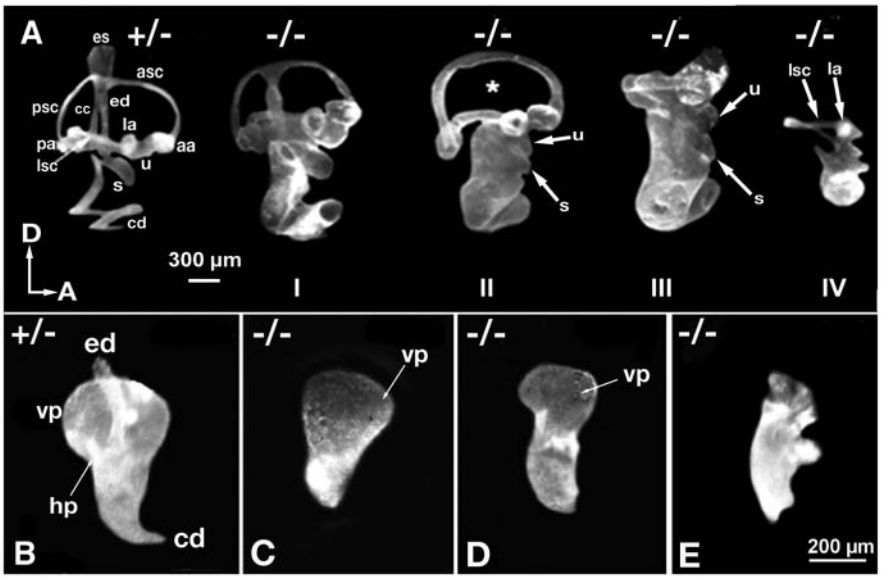

Fig. 2. Paint-filled inner ears of *Gbx2* mutants. Lateral views of right inner ears from heterozygous and homozygous *Gbx2* embryos at 15.5 (A) and 11.5 dpc (B-E). (A) The control inner ear is shown on the left followed by four representative phenotypes, shown with increasing severity from Type I to IV. Type I: an enlarged membranous labyrinth lacking the endolymphatic duct (ed). Type II: absence of both the endolymphatic duct and common crus (cc, asterisk). The utricle (u) and saccule (s) are not easily discernible, and the cochlear duct is shortened. Type III: the inner ear is missing the anterior and posterior canals, in addition to phenotypes described for Type II. Type IV: a cystic inner ear with only the lateral canal and ampulla. (B) A normal inner ear at 11.5 dpc. (C-E) *Gbx2* mutant ears with a normal (C), smaller (D) or non-existent (E) vertical canal pouch. asc, anterior semicircular canal; cc, common crus; cd, cochlear duct; ed, endolymphatic duct; es, endolymphatic sac; hp, horizontal canal pouch; lsc, lateral semicircular canal; psc, posterior semicircular canal; s, saccule; u, utricle; vp, vertical canal pouch. Scale bar in E applies to B-E.

Paint-fill analysis of *Gbx2* mutant inner ears

Next, we investigated the gross anatomy of *Gbx2*$^{-/-}$ inner ears at 15.5 dpc using the paint-fill technique (Fig. 2). A total of 19 homozygous mutant embryos were analyzed, and a repertoire of phenotypes was observed. We divided the specimens into four categories (I, II, III and IV), based on the severity of the phenotype (Fig. 2, Table 1). Overall, *Gbx2* mutant inner ears are usually missing the endolymphatic duct (Table 1, *n*=18/19), with an enlarged membranous labyrinth (Fig. 2A). By contrast, the lateral canal and ampulla are usually present (Table I, *n*=17/19). Type I, the mildest phenotype, shows an enlarged membranous labyrinth, and three out of the four specimens are missing the endolymphatic duct (Table 1). In the Type II category, most of the inner ears are missing the common crus (Fig. 2A, asterisk; *n*=5/7), in addition to the absence of the endolymphatic duct (*n*=7/7). The utricle and saccule are not easily discernible, and the saccule is often fused with the cochlear duct. In the Type III inner ears, the anterior and posterior semicircular canals are also missing but the lateral canal is present (*n*=3). The cochlear ducts of Type III specimens are more malformed than those of Type I and Type II, and have less than one coil. Inner ears categorized as Type IV are the most severe; they are cystic without any discernible structures except for the presence of the lateral canal in some cases (*n*=3/5). Taken together, the lack of *Gbx2* function affects inner ear structures such as canals and cochlear duct that do not express *Gbx2* (Fig. 1; Table 1), suggesting that *Gbx2* has a non-cell autonomous role in inner ear development. Despite the variable phenotypes among the *Gbx2* mutants, the two ears of a given specimen usually display similar phenotypes (*n*=8/10).

Vertical canal pouch formation in *Gbx2* mutants

Approximately half of the specimens in *Gbx2* mutant inner ears are missing the anterior and posterior canals, as well as the common crus (Table 1). The anterior and posterior canals form from a vertical outpouch in the dorsal region of the otocyst (Fig. 2B, VP). Over time, the opposing epithelia in the center region of each presumptive canal approach each other, fuse and reabsorb, leaving behind the two canals connected by the common crus. This morphogenetic process is completed by 13 dpc in mice (Fig. 2A) (Morsli et al., 1998). The absence of the canals and common crus in *Gbx2* mutants could be due to a failure of canal pouch formation. Alternatively, excessive epithelial resorption could eliminate the epithelia that normally form the canals and common crus. To further investigate these two possibilities, we examined 11 paint-filled ears during canal pouch development between 11 and 12 dpc (seven embryos between 11 and 11.5 dpc; four embryos between 12 and 12.75 dpc). Figure 2C-E illustrate three paint-filled inner ears at 11.5 dpc with a normal (Fig. 2C), a small (Fig. 2D) or a non-existent (Fig. 2E) vertical canal pouch. Interestingly, 45% of these specimens between 11 and 12 dpc have either no or a small

Table 1. Affected inner ear structures in *Gbx2* homozygotes

	Number affected*				% of total mutants lacking specific structures
	Type I (*n*=4)	Type II (*n*=7)	Type III (*n*=3)	Type IV (*n*=5)	
ED/ES	3(3)	7(7)	3(3)	5(5)	95% (18/19)
ASC	3(0)	7(0)	3(3)	5(5)	42% (8/19)
PSC	3(0)	7(0)	3(3)	5(5)	42% (8/19)
LSC	3(0)	7(0)	3(0)	5(2)	11% (2/19)
CC	4(0)	7(5)	3(3)	5(5)	68% (13/19)
AA	1(0)	7(0)	3(1)	5(3)	21% (4/19)
PA	0(0)	7(0)	3(1)	5(3)	21% (4/19)
LA	1(0)	7(0)	3(0)	5(2)	11% (2/19)
Utricle	4(0)	7(0)	3(0)	5(0)	0% (0/19)†
Saccule	4(1)	7(1)	3(2)	5(4)	42% (8/19)
CD	4(0)	7(0)	3(0)	5(5)	26% (5/19)

*Total number of specimens with malformation of specific structures, including membranous swelling. Numbers within the brackets represent the number of specimens missing specific structures.

†As the utricle is part of the inner ear proper, it is difficult to determine if the structure is missing or poorly developed.

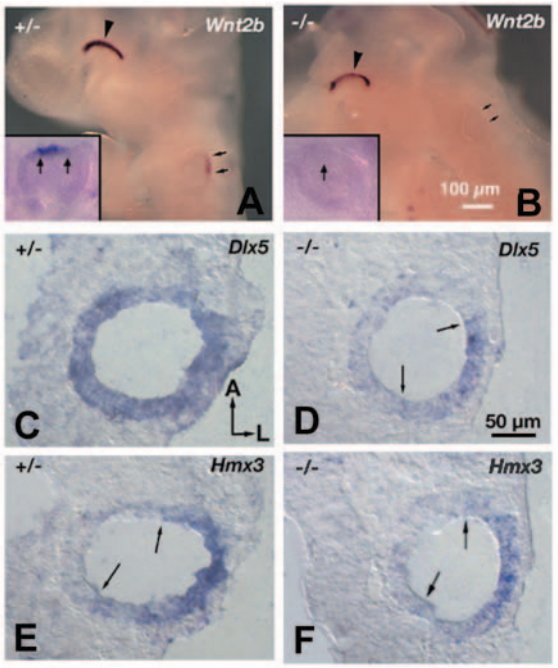

Fig. 3. Gene expression analyses of *Gbx2* mutants. Whole mounts of heterozygous (A) and homozygous (B) *Gbx2* embryos probed for *Wnt2b* transcripts at 10 dpc. Arrows indicate the presence or absence of *Wnt2b* expression in the otocyst. An arrowhead indicates *Wnt2b* expression in the eye. Inserts in A and B show +/– (A) and –/– (B) otocysts at 9.5 dpc that have undergone prolonged color development. (C-F) Cryosections probed for *Dlx5* (C,D) and *Hmx3* (E,F) transcripts at 9.5 dpc. Pairs of 12 μm adjacent sections from +/– (C,E) and –/– (D,F) *Gbx2* inner ear. (C) *Dlx5* is expressed in the entire dorsal region of a +/– otocyst, whereas *Hmx3* is expressed only in the lateral region (E, arrows). (D,F) In a –/– otocyst, the medial expression domain of *Dlx5* is absent, whereas both *Dlx5* and *Hmx3* are expressed in the lateral regions. Arrows in D-F indicate the borders of expression domains. Scale bars: in B, 100 μm for A,B; in D, 50 μm for C-F.

vertical canal pouch. This percentage corresponds well to the 42% of the specimens missing anterior and posterior canals at 15.5 dpc (Table 1), suggesting that the canal defect originates during the canal pouch outgrowth stage. Whether mis-regulated epithelial resorption is also involved in the phenotype is not clear. In addition to the canal pouch defects, the lack of the endolymphatic duct and cochlear duct extension is also evident by 11.5 dpc (Fig. 2C-E).

Loss of endolymphatic duct markers in *Gbx2* mutant inner ears

The most prevalent phenotype of the *Gbx2* mutants, the absence of the endolymphatic duct, was examined in more detail using gene expression analyses. *Wnt2b* is normally expressed in the endolymphatic duct, and its expression is initiated in the dorsal pole of the otocyst starting at 9.5 dpc (Fig. 3A) (Riccomagno et al., 2002). *Wnt2b* expression is not detected in otocysts of *Gbx2* mutants at 9.5 or 10 dpc, suggesting a failure of endolymphatic duct specification (Fig. 3B; *n*=4).

In a normal otocyst at 9.5 dpc, *Dlx5* is expressed in the entire dorsal region of the otocyst (Fig. 3C), whereas *Hmx3* is expressed in the lateral region only (Fig. 3E). Consistent with the expression patterns in the otocyst, in a more mature inner ear, *Dlx5* is expressed in both dorsal structures including the endolymphatic duct and the semicircular canals (Acampora et al., 1999; Depew et al., 1999; Merlo et al., 2002). However, *Hmx3* is only expressed in the canals, which are dorsolateral structures (Rinkwitz-Brandt et al., 1996; Rinkwitz-Brandt et al., 1995). Therefore, we extrapolated from these results that the dorsomedial domain of the otocyst that is *Dlx5* positive and *Hmx3* negative, gives rise to the endolymphatic duct; the dorsolateral domain that is positive for both *Dlx5* and *Hmx3*, gives rise to the three semicircular canals. This idea is supported by results from knockout mouse studies showing that *Dlx5* is important for both endolymphatic duct and canal development, whereas *Hmx3* is primarily required for canal formation (Acampora et al., 1999; Depew et al., 1999; Hadrys et al., 1998; Wang et al., 1998). According to the proposed boundary model of cell fate specification in the inner ear (Fekete, 1996; Kiernan et al., 1997) the absence of *Gbx2* could affect the normal boundaries of *Dlx5* and *Hmx3* expression domains, leading to malformations of both the endolymphatic duct and semicircular canals. In the *Gbx2* mutants, there is a loss of *Dlx5* expression in the medial region of the otocyst but its expression in the lateral region remains (Fig. 3D, arrows; *n*=4), suggesting *Gbx2* is required to maintain *Dlx5* expression only regionally. Despite the loss of *Dlx5* in the medial otocyst, there is no expansion of the *Hmx3* expression domain medially (Fig. 3F, arrows; *n*=4). Therefore, these results suggest that the failure of endolymphatic duct specification in *Gbx2* mutants is not due to a change in domain boundaries, but rather a change in the induction and/or maintenance of the expression of genes such as *Wnt2b* and *Dlx5*. In addition, these gene expression changes in the mutants are not associated with an obvious change in either cell proliferation or apoptosis in the dorsomedial region of the otocyst at this age (data not shown).

Ganglion and sensory organ development in *Gbx2* mutants

Despite the fact that *Gbx2* is not normally expressed in the *Lfng*-positive neurogenic and sensory competent region (Fig. 1F,G), the variable and sometimes severe phenotypes observed in *Gbx2* mutants suggest that the development of this region is also affected. We examined ganglion and sensory organ formations in *Gbx2* mutants at 15.5 dpc using in situ hybridization. Owing to the variability of phenotypes, cryosections from each *Gbx2* specimen were partially reconstructed and categorized as Type I to Type IV. A total of seven *Gbx2* mutant ears were analyzed for the presence of vestibular and spiral ganglia (Type I, *n*=2; Type II, *n*=3; and Type IV, *n*=2) using RNA probes for *Nf68* and *Gata3* transcripts. The vestibular ganglion is present in the mutant ears of all phenotypes examined (Fig. 4A,B). The spiral ganglion is present in most of the Type II specimens (Fig. 4C,D; *n*=2/3) but missing in both Type IV specimens.

To investigate the cause for the ganglion defect, we examined the delamination of the neuroblasts at E10.5 based on the expression pattern of *Neurod1* (Fig. 4E,F; *n*=6). Neuroblasts appear to delaminate normally in the *Gbx2* mutants, but there is an increased number of apoptotic cells in the delaminated neuroblasts between 9.5 and 10.5 dpc compared with normal (Fig. 4G,H; *n*=5). This increase in cell

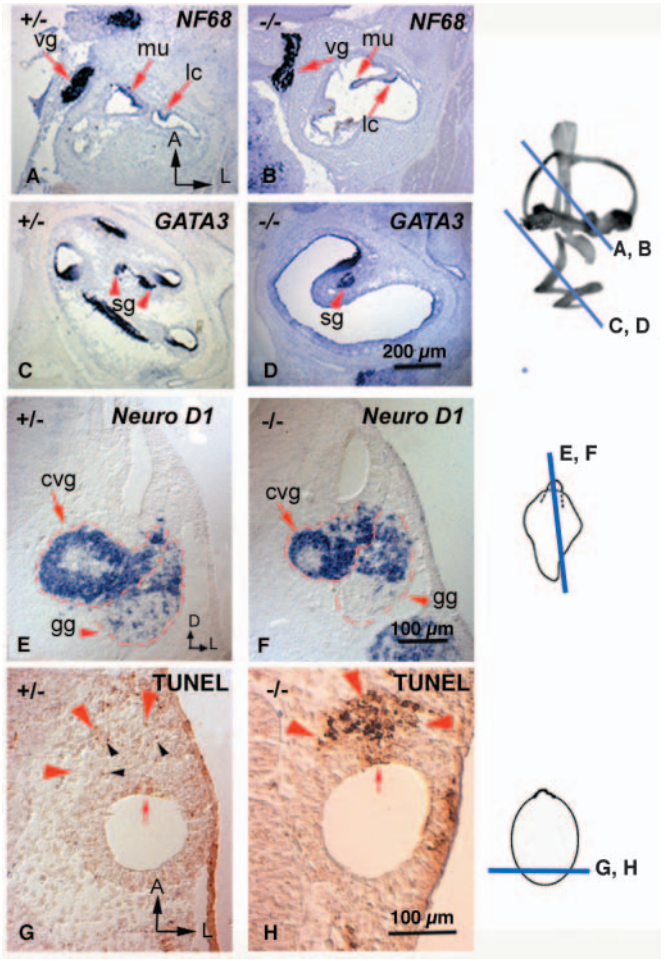

Fig. 4. Ganglion formation in *Gbx2*$^{-/-}$ inner ears. Heterozygous (A,C,E,G) and homozygous (B,D,F,H) *Gbx2* inner ears probed for *Nf68* (A,B) *Gata3* (C,D) and *Neurod1* (E,F) transcripts, and apoptotic cells (G,H) at (A-D) 15.5, (E,F) 10.5 and (G,H) 9.5 dpc. (G,H) TUNEL analyses show an increased in apoptotic cells in the cochleo-vestibular ganglion (G,H, red arrowheads) of a –/– otocyst (H) compared with a +/– otocyst (G, black arrowheads). Arrows indicate a region of cell death within the otic epithelium of +/– and –/– inner ears. cvg, cochleo-vestibular ganglion; gg, geniculate ganglion; sg, spiral ganglion; vg, vestibular ganglion. Schematics on the right indicate the levels of sections. Scale bars: in D, 200 μm for A-D; in F, 100 μm for E,F; in H, 100 μm for G,H.

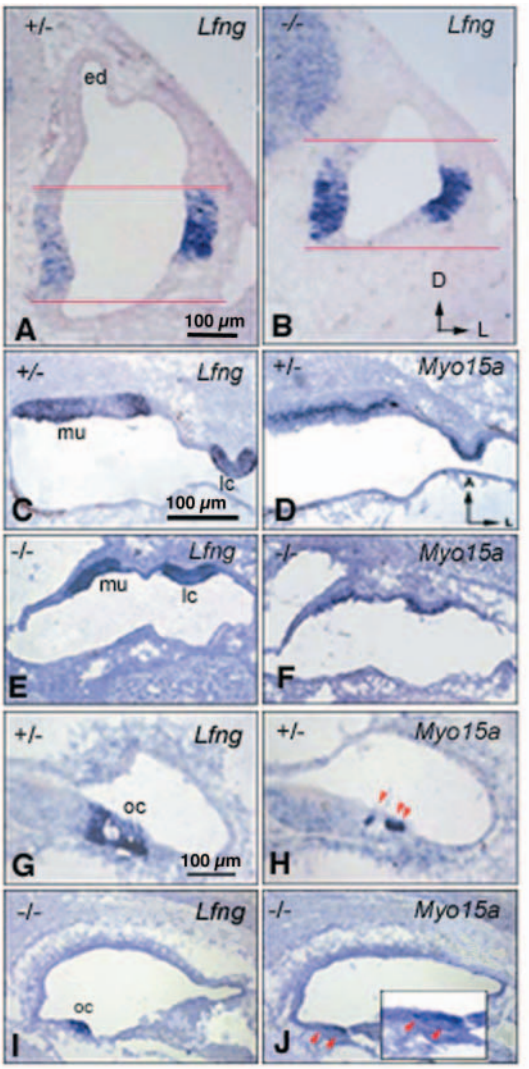

Fig. 5. Sensory organ formation in *Gbx2*$^{-/-}$ inner ears. Sections of heterozygous (A,C,D,G,H) and homozygous (B,E,F,I,J) *Gbx2* inner ears probed for *Lfng* or *Myo15a* transcripts at 10.5 (A,B) and 15.5 (C-J) dpc. (C-J) Pairs of 12 μm adjacent sections. Red lines indicate comparable *Lfng* expression domains between +/– and –/– ears. *Lfng* (E) and *Myo15a* (F) are expressed in the lateral crista (lc) and macula utriculi (mu) of a Type IV *Gbx2*$^{-/-}$ inner ear. Arrowheads in H indicate the sensory hair cells. Only one or two *Lfng*- (I) and *Myo15a* (J)-positive sensory patches are present in a Type II *Gbx2*$^{-/-}$ cochlear duct. Insert in J shows a higher power view of the *Myo15a* positive sensory region. Arrowheads indicate the region that is positive for both *Lfng* and *Myo15a*. Scale bars: in A, 100 μm for A,B; in C, 100 μm for C-F; in G, 100 μm for G-J.

death could contribute to the ganglion phenotype observed at later stages.

The *Lfng* expression domain that encompasses the neurogenic/sensory region appears normal in the *Gbx2* mutants at 10.5 dpc (Fig. 5A,B, area between the red lines; n=3). However, based on the 3-D reconstruction of serial sections, the otic region dorsal to the *Lfng* domain is smaller, suggesting that this region is underdeveloped in *Gbx2* mutants (Fig. 5A,B).

Despite the normalcy of the *Lfng* domain at 10.5 dpc, sensory organ formation is variable, particularly among the ventral sensory organs (Table 2). At 15.5 dpc, the lateral crista is found in all the specimens examined, consistent with the paint-fill results (Fig. 5C,E; Table 2). In addition, a sensory patch that corresponds to the position of the macula utriculi is also present, even in the most severely affected ears (Fig. 5C,E). Both the lateral crista and macula utriculi express a sensory hair cell-specific gene, *Myo15a* (Fig. 5D,F). Anterior and posterior cristae are generally present, except in some of the Type IV ears. The ventral sensory patches, however, such as the macula sacculi and organ of Corti, are severely affected in most mutants (Table 2). No discernible sensory patches for the macula sacculi can be positively identified even in the Type

Table 2. Analysis of sensory patches in *Gbx2*$^{-/-}$ inner ears at 15.5 dpc

Specimen	Type	AC	PC	LC	MU	MS	OC
et486B/l	I	+	+	+	+	+	+
et486C/r	I	+	+	+	+	+	+*
et863C/r	I	+	+	+	+	+	+*
326D/r	II	+	+	+	+	U.I.	+*
334B/r	II	+	+	+	+	U.I.	+*
334A/r	III	+	+	+	+	U.I.	+*
352A/r	IV	+	–	+	+†	–	+*
352D/r	IV	–	–	+	+	–	+*

U.I., Unidentifiable, small or not a separate entity; +, presence of specific sensory patches based on *Lfng* expression.
*The presence of only one or two small *Lfng*-positive patches.
†Small sensory patch.

II ears, and the cochlear ducts usually consist of one or two small sensory patches that express a hair cell-specific marker, *Myo15a* (Fig. 5G-J).

Expansion of *Otx2* expression domain in *Gbx2*$^{-/-}$ inner ears

We further investigated the cause for the poorly developed ventral sensory structures. *Eya1*, *Gata3* and *Pax2* are all important for the normal development of the cochlear duct (Burton et al., 2004; Karis et al., 2001; Torres et al., 1996; Xu et al., 1999). Expression patterns of these three genes were examined in the cochlear duct of *Gbx2* mutants, but none were changed significantly to provide any insight into the cause of the cochlear malformation. As there is good evidence that *Gbx2* and *Otx2* negatively regulate each other in the mid-hindbrain region, we examined the expression of *Otx2* in *Gbx2*$^{-/-}$ inner ears.

At 10.5 dpc, *Otx2* is normally expressed in the ventral posterolateral region of the otic vesicle, and its expression is complementary to the *Lfng* domain (Fig. 6A-D). In the *Gbx2* mutants, the dorsal region of the *Otx2* expression domain is fairly normal, but ventrally its expression expands medially into the *Lfng* domain (Fig. 6E-H, brackets; six otocysts from four embryos). The extent of the *Otx2* expression domain expansion is variable among specimens. One ear from one embryo shows medial expansion of the entire *Otx2* expression domain, while another specimen shows a normal expression domain. Both of these specimens show variability between left and right ears. This aberrant expression of *Otx2* in the ventromedial region is also observed at later stages, even though the extent of *Otx2* domain expansion varies between specimens (Fig. 6I, double arrows; Fig. 6J-L; arrows; n=8 between 11.5 to 15.5 dpc). Interestingly, unlike the situation in the mid-hindbrain region, the *Gbx2* expression domain in a normal mouse inner ear does not abut the *Otx2* domain (Fig. 6M-N). Similar expression patterns have been reported in the chicken inner ear (Hidalgo-Sanchez et al., 2000).

Abnormalities in the caudal hindbrain of *Gbx2* null mutants

Next, we assessed between 9 and 9.5 dpc the integrity of the hindbrain region (r4-r6) that is closest to the developing inner ear. It has been shown that the anterior hindbrain rostral to r4 is missing in the *Gbx2* mutants and is replaced by an ill-defined zone with aberrant gene expression patterns (Wassarman et al., 1997). Gene expression patterns caudal to r4 have not been reported in detail. At 9 to 9.5 dpc, *Krox20* (*Egr2* – Mouse Genome Informatics) and *Epha4* are normally expressed in r3 and r5. In *Gbx2* mutants, the levels of both *Krox20* and *Epha4* expression in r5 are reduced compared with heterozygotes (Fig. 7A-D; n=4). Note the smaller size of the otocysts in some *Gbx2* mutants (Fig. 7D, arrows). However, *Hoxb1*, a marker for r4, is expressed in its normal position relative to the otocyst,

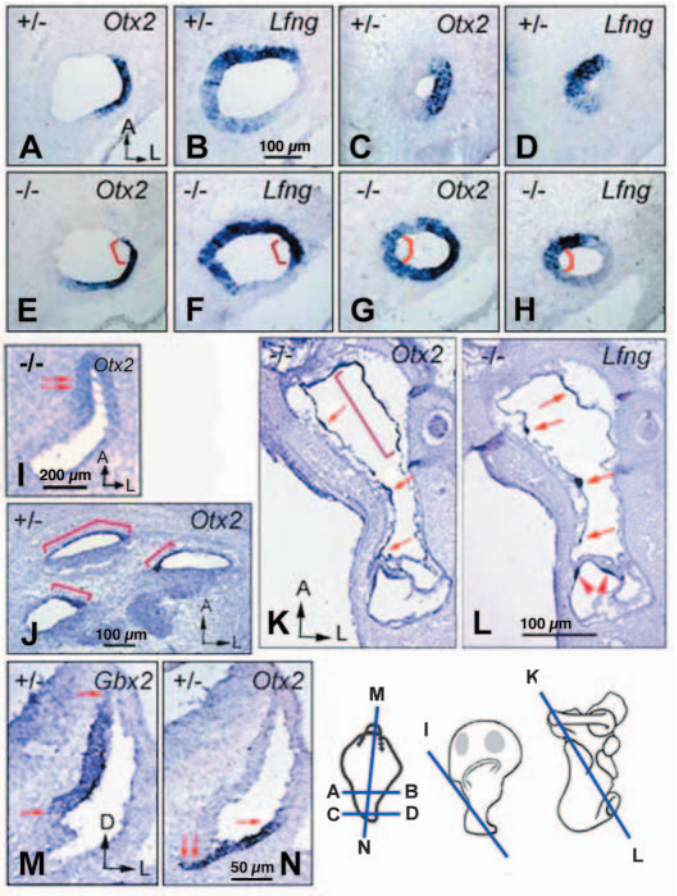

Fig. 6. Aberrant *Otx2* expression in *Gbx2* mutants. *Otx2* (A,C,E,G) and *Lfng* (B,D,F,H) expression patterns in heterozygous (A-D) and homozygous (E-H) *Gbx2* inner ears. (A,B and E,F) Comparable pairs of 12 μm adjacent sections dorsal to the pairs shown in C,D and G,H respectively. *Otx2* and *Lfng* expression domains are complementary in heterozygous, but overlap with each other in homozygous *Gbx2* otocysts (brackets). (I) The *Otx2* expression domain expands medially in the growing cochlear duct of *Gbx2*$^{-/-}$ ears at 12 dpc (double arrows). (J-L) Comparable cochlear sections at 15.5 dpc. (J) *Otx2* expression in the Reissner's membrane of a +/– cochlear duct (bracket). (K,L) Adjacent cochlear sections of *Gbx2*$^{-/-}$ mutants probed for *Otx2* (K) and *Lfng* (L) transcripts. A bracket in K marks the normal *Otx2* expression domain and arrows indicate ectopic *Otx2* expression in the medial region. Arrows in L indicate a *Lfng*-positive sensory region in the cochlea, and arrowheads indicate the sensory region in the posterior crista. (M,N) Adjacent +/– inner ear sections at 10.5 dpc probed for *Gbx2* (M) and *Otx2* (N) transcripts. Arrows indicate the borders of expression domain for each gene, and double arrows indicate the lateral restriction of *Otx2* expression domain. Schematics on the right indicate the levels of sections. Scale bars: in B, 100 μm for A-H; in L, 100 μm for L,K; in N, 50 μm for M,N.

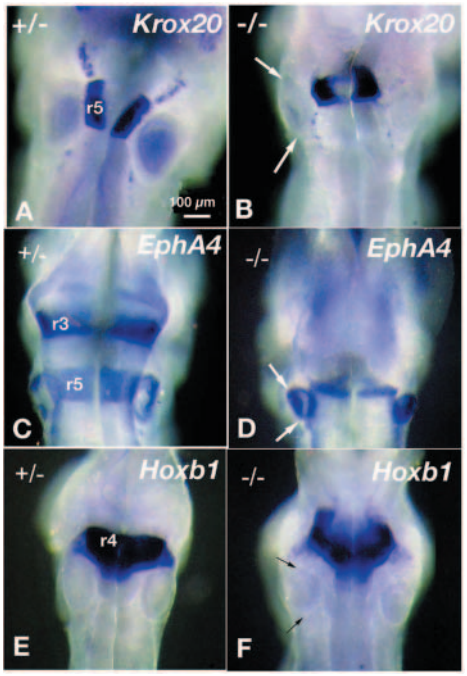

Fig. 7. Analysis of hindbrain markers in *Gbx2*$^{-/-}$ inner ears. Dorsal views of +/– (A,C,E) and –/– (B,D,F) *Gbx2* embryos probed for *Krox20* (A,B), *Epha4* (C,D) and *Hoxb1* (E,F) RNA transcripts at 9 dpc. In *Gbx2*$^{-/-}$ embryos, *Krox20* (B) and *Epha4* (D) expression domains are reduced in r5, and the anterior border of *Hoxb1* expression domain (F) is aberrant. Arrows indicate the borders of otocysts. Scale bar in A: 100 μm for A-F.

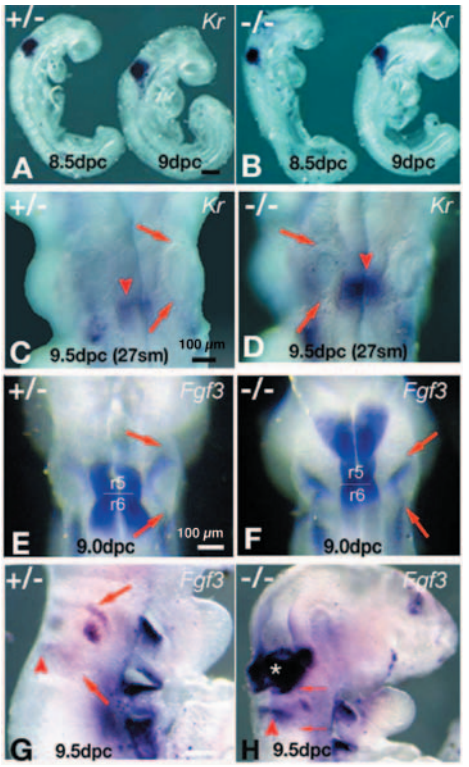

Fig. 8. Expression patterns of *Fgf3* and kreisler/*Mafb* in *Gbx2*$^{-/-}$ embryos. Lateral (A,B) and dorsal (C,D) views of the kreisler/*Mafb* expression pattern in the hindbrain of *Gbx2*$^{+/-}$ (A,C) and –/– (B,D) embryos. (A,B) No obvious difference in kreisler/*Mafb* expression pattern is observed between +/– and –/– embryos before 9.0 dpc. (C,D) By 9.5 dpc, kreisler/*Mafb* is expressed weakly in r6 of +/– (C, arrowhead) and much more strongly in –/– (D) embryos. (E,F) Dorsal and (G,H) lateral views of the *Fgf3* expression patterns in the hindbrains of heterozygous (E,G) and homozygous (F,H) *Gbx2* mutants. (E,F) At 9.0 dpc, the *Fgf3* expression domain extends beyond r5 and r6 into r4 and possibly includes the undefined region rostral to r4 in *Gbx2*$^{-/-}$ embryos. (G,H) By 9.5 dpc, *Fgf3* expression is no longer detectable in the hindbrain (G) but is strong in r4 and rX (asterisk) and weaker in r6 (arrowhead) of *Gbx2*$^{-/-}$ embryos (H). The *Fgf3* expression patterns in both otocysts (G,H) are comparable in the anteroventral lateral region. Arrows in C-H mark the anterior and posterior margin of the otocyst. sm, somite pairs. Scale bars: in A, 100 μm for A,B; in C, 100 μm for C,D; in E, 100 μm for E-H.

except that the rostral boundary of its expression domain is not as well-defined as controls (Fig. 7E,F; *n*=2).

As kreisler/*Mafb* and *Fgf3* have been implicated in inner ear development, we examined in more detail the expression patterns of these two genes in *Gbx2* mutants. kreisler/*Mafb* is expressed in the presumptive r5 and r6, starting at 8.0 dpc (Cordes and Barsh, 1994) (Fig. 8A), and its expression is downregulated in the hindbrain, with a weak expression in r6 by late 9.5 dpc (Fig. 8C, arrowhead). In *Gbx2* mutants, there is no difference in kreisler/*Mafb* expression up to 9.5 dpc (Fig. 8B; *n*=3). However, by late 9.5 dpc (27 somites), kreisler/*Mafb* is still expressed in r6, while it is downregulated in controls by this stage (Fig. 8C,D; *n*=2).

Fgf3 is normally expressed in the hindbrain beginning at 8 dpc (four somites) (Mahmood et al., 1996; McKay et al., 1996). From 8.5 dpc to 9 dpc, the expression of *Fgf3* in r5-r6 is high, and then subsides by 9.5 dpc (Fig. 8E,G). In the *Gbx2* mutants, *Fgf3* is strongly expressed in r5 and r6 (Fig. 8F). In addition, its expression domain extends into r4 and possibly to the undefined region rostral to r4 (*n*=4). By late 9.5 dpc, *Fgf3* expression in normal hindbrain is barely detectable (Fig. 8G), whereas in *Gbx2* mutants, *Fgf3* expression in r6 persists (Fig. 8H, arrowhead). Strong expression of *Fgf3* is observed also in r4, and possibly the region rostral to r4 (Fig. 8H, asterisk; *n*=3). Despite these aberrant gene expression patterns in the hindbrain, the *Fgf3* expression in the anterolateral region of the otocyst in *Gbx2* mutants is normal (Fig. 8G,H). Taken together, loss of *Gbx2* function in the neural tube evidently affects the development of the caudal hindbrain, which in turn may affect inner ear development. However, hindbrain genes such as kreisler/*Mafb* and *Fgf3* that have been implicated in inner ear development are upregulated in the hindbrain rather than downregulated.

Discussion

The role of *Gbx2* in patterning dorsal inner ear structures

Our results demonstrate that *Gbx2* is required for the formation of the endolymphatic duct, a dorsomedial structure. In the *Gbx2* mutants, expression patterns of both *Wnt2b* and *Dlx5* are affected in the presumptive endolymphatic duct region. As *Gbx2* is normally expressed in this region, *Gbx2* is probably required cell autonomously for endolymphatic duct formation. By contrast, *Gbx2* has a non-cell autonomous role in canal

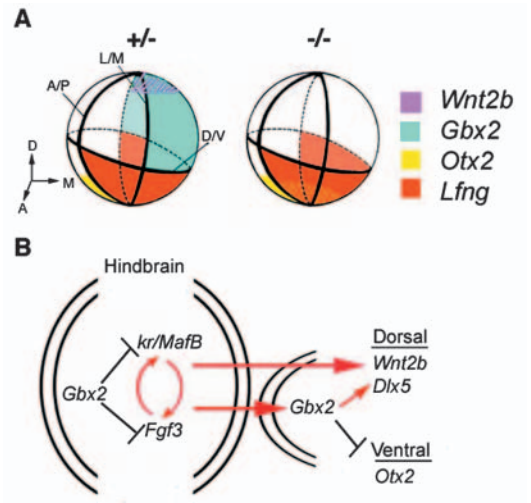

Fig. 9. A summary of (A) gene expression changes in *Gbx2* mutants and (B) proposed interactions of *Gbx2* with other genes known to affect inner ear development. (A) Anterior views of a schematic $Gbx2^{+/-}$ and $Gbx2^{-/-}$ right otocyst. *Gbx2* is expressed in the dorsomedial domain (blue); *Lfng* is expressed in the anteroventral lateral domain that expands medially (orange); and *Otx2* is expressed in the ventral posterolateral domain (yellow) that is complementary to the *Lfng* domain and non-abutting to the *Gbx2* domain. In a homozygous mutant, there is a loss of *Wnt2b* expression (purple) and *Dlx5* expression dorsomedially (not shown), as well as an expansion of *Otx2* expression domain ventromedially (yellow color). (B) Possible relationships of *Gbx2* with other genes in the hindbrain and inner ear. Arrows do not imply direct interactions.

development. The lack of *Gbx2* affects the formation of the vertical canal pouch that develops into the anterior and posterior canals, two dorsolateral structures. How *Gbx2* mediates this non-cell autonomous function remains an unanswered question. *Gbx2* in the dorsomedial region of the otocyst could induce a signaling molecule that patterns neighboring cells in the dorsolateral region. Alternatively, some long-range signaling molecules from the hindbrain, which are perturbed in the *Gbx2* mutants, could be directly responsible for the development of the vertical canal pouch. Interestingly, the formation of a lateral structure, the lateral canal is usually not affected by the lack of *Gbx2*.

The role of *Gbx2* in patterning ventral inner ear structures

Gbx2 also has a non-cell autonomous role in patterning ventral inner ear structures such as the saccule and cochlea. In the developing neural tube, the rostral expression domain of *Gbx2* and the caudal expression domain of Otx2 form a sharp border that dictates the position of the mid-hindbrain junction within the neural tube. Ectopic expression studies indicate that these two genes antagonize the expression of one another to form this sharp border (Broccoli et al., 1999; Millet et al., 1999). A similar antagonistic relationship between Gbx2 and Otx2 could be occurring in the inner ear. However, unlike the mid-hindbrain junction, the expression domains of *Gbx2* and *Otx2* in the inner ear do not abut each other. Although *Gbx2* is expressed in the dorsal medial region of the otic vesicle, *Otx2* is expressed in the ventral posterolateral region. Sandwiched in between the two domains is the *Lfng*-positive sensory competent region that is negative for both *Gbx2* and *Otx2* (Fig. 9A). Here, we show that the *Lfng* domain appears to form normally in the *Gbx2* mutants. However, the lack of *Gbx2* results in an expansion of *Otx2* domain medially and possibly affects the subsequent development of the *Lfng* positive, sensory region (Fig. 9A). This aberrant expression of *Otx2* in the ventral region is not observed in other knockout mice with cochlear defects such as sonic hedgehog and *Pax2* knockout mice (Burton et al., 2004; Riccomagno et al., 2002). Given the known functions of Otx2 in regional identity in other systems (Acampora et al., 1995; Ang et al., 1996; Rhinn et al., 1998), the ectopic *Otx2* expression in the inner ear of *Gbx2* mutants could be causal to the ventral defects observed. Interestingly, the lack of the endolymphatic duct in mice is invariably associated with defects in other parts of the inner ear (Fekete, 1999; Kiernan et al., 2002), possibly owing to loss of *Gbx2* expression. This suggests that a disrupted relationship between *Gbx2* and *Otx2* expression patterns could be a common molecular mechanism underlying other inner ear defects in mouse mutants lacking an endolymphatic duct. This hypothesis needs to be tested directly in other experimental paradigms.

The cause for the increased apoptosis in the delaminated neuroblasts is unclear as *Gbx2* expression is not detected in the cochleovestibular ganglion. Nevertheless, this observed cell death could attribute to the ganglion phenotype observed at later stages. In addition, the reduction or absence of the spiral ganglion in some specimens could also be caused by a reduction in the supply of neurotrophins from the poorly developed sensory tissues.

The role of *Gbx2* in the hindbrain

In the hindbrain of *Gbx2* mutants, we observed a change in gene expression patterns caudal to r3, in addition to defects described for the anterior hindbrain (Wassarman et al., 1997). We show that r5 is abnormal based on *Krox20* and *Epha4* expression patterns. The size of r4 appears relatively normal, but *Fgf3* is ectopically expressed in this region. In addition, the temporal expression patterns of both kreisler/*Mafb* and *Fgf3* are prolonged in r6. These results suggest that *Gbx2* is required for normal development of the caudal hindbrain; it regulates the temporal expression of kreisler/*Mafb* and *Fgf3* and maintains the expression of *Krox20* and *Epha4*. However, many of these affected genes are thought to regulate each other in the hindbrain (Theil et al., 2002; Theil et al., 1998). For example, ectopic expression of kreisler/*Mafb* in r3 and r5 results in an upregulation of *Fgf3* in these rhombomeres (Theil et al., 2002). However, in chicken, the loss of FGF signaling using an inhibitor of the FGF receptor abolishes kreisler/*Mafb* expression in the hindbrain (Marin and Charnay, 2000). These results suggest that kreisler/Mafb and FGF3 positively regulate each other. Furthermore, ectopic expression of *Mafb* also represses the expression of both *Krox20* and *Epha4* in the chicken hindbrain (Giudicelli et al., 2003). Taken together, these results suggest that the downregulation of *Krox20* and *Epha4* in *Gbx2* mutants is mediated by the upregulation of kreisler/*Mafb* and/or *Fgf3*.

Inner ear *Gbx2* expression is downstream of hindbrain signaling

Signaling from the hindbrain plays an important role in inner

ear development. As *Gbx2* is expressed in both the hindbrain and inner ear itself, the inner ear phenotypes observed in the *Gbx2* knockout mice might be due to disrupted hindbrain formation and signaling and/or the lack of *Gbx2* activity within the inner ear.

We postulate that *Gbx2* expression in the inner ear is a primary downstream target of hindbrain signaling (Fig. 9B). Several lines of evidence support this hypothesis. First, kreisler/*Mafb* expression in the hindbrain at 7.5 dpc precedes *Gbx2* expression in the inner ear at 8.5 dpc. Second, the downregulation of *Gbx2* expression in the inner ears of *kreisler* mice strongly supports the notion that expression of *Gbx2* in the inner ear is regulated by the kreisler/*Mafb* pathway (D. Choo, personal communication). Third, hindbrain rotation experiments in chicken indicate that the maintenance of otic *Gbx2* expression is dependent on signaling from the hindbrain (Bok et al., 2004). Fourth, there is a strong resemblance in the inner ear phenotypes described here for the *Gbx2* mutants and those described for *kreisler* (D. Choo, personal communication). In *kreisler*, the endolymphatic duct fails to develop, and the lateral ampulla and canal are the least affected structures, similar to the *Gbx2* mutants. Finally, similar molecular changes such as ectopic expression of *Otx2* and downregulation of *Dlx5* are also observed in *kreisler* mutants (D. Choo, personal communication). It remains to be determined, however, whether other hindbrain mutants such as *Hoxa1* knockout mice show similar gene expression changes as we have observed for *Gbx2* mutants.

Other evidence supports the idea that *Gbx2* expression in the inner ear is a more important requirement for inner ear development than *Gbx2* expression in the hindbrain. *Fgf3* expression in the hindbrain is prolonged in the *Gbx2* mutants. It has been shown that ectopic expression of *Fgf3* in the hindbrain of chicken resulted in a distended endolymphatic duct (Vendrell et al., 2000). Therefore, the prolonged expression of *Fgf3* in the hindbrain of *Gbx2* mutants could have resulted in a larger endolymphatic duct, but this is not the case. The lack of an endolymphatic duct phenotype in *Gbx2* mutants is more consistent with a loss rather than a gain of *Fgf3* function. These results, however, could be reconciled if kreisler/*Mafb* and/or *Fgf3* in the hindbrain normally induce or maintain *Gbx2* expression in the inner ear. Then, the absence of *Gbx2* within the inner ear would negate any phenotype caused by the upregulation of either kreisler/*Mafb* or *Fgf3* and would result in a phenotype that resembles a loss of kreisler function.

Although we postulate that the majority of the inner ear phenotype is due to the loss of *Gbx2* expression within the inner ear, any of the gene expression changes observed in the hindbrain of *Gbx2* mutants could also contribute to the inner ear phenotype. No inner ear malformations due to the lack of *Krox20* and *Epha4* have been reported (Dottori et al., 1998; Sham et al., 1993; Swiatek and Gridley, 1993). Even though the role of *Wnt2b* in inner ear development is not known, the absence of *Wnt2b* expression in *Gbx2* mutants could be due to gene expression changes at the level of the hindbrain because the expression patterns of *Wnt2b* and *Gbx2* within the inner ear appear to be independently regulated (Riccomagno et al., 2002). A tissue-specific knockout of *Gbx2* only in the inner ear or hindbrain should determine which source of *Gbx2* is more important for inner ear development.

Under the assumption that *Gbx2* in the inner ear is a major downstream target of signaling from the hindbrain, this *Gbx2* expression domain probably mediates hindbrain signaling by maintaining expression of genes such as *Dlx5* to promote formation of dorsal structures (Fig. 9). However, its role in ventral patterning is inhibitory and possibly mediated by restriction of *Otx2* expression. This proposed inhibitory role of *Gbx2* is different from the postulated inductive role of sonic hedgehog, another signaling molecule that emanates from the hindbrain and notochord, and induces or maintains expression of genes such as *Otx2* and *Pax2* (Riccomagno et al., 2002). *Otx1*, *Otx2* and *Pax2* are all required for the normal development of the saccule and cochlear duct (Burton et al., 2004; Cantos et al., 2000; Morsli et al., 1999). Multiple inductive and inhibitory molecules at the level of transcriptional control are likely to be involved in achieving the formation of an intricate organ such as the inner ear, and this paper presents insight into such a mechanism.

We are indebted to Dr Daniel Choo for discussion and sharing experimental results prior to publication, to Dr Alex Joyner for the $Gbx2^{+/-}$ mice, and to Drs Susan Sullivan and Thomas Friedman for critical reading of the manuscript.

References

Acampora, D., Mazan, S., Lallemand, Y., Avantaggiato, V., Maury, M., Simeone, A. and Brulet, P. (1995). Forebrain and midbrain regions are deleted in $Otx2^{-/-}$ mutants due to a defective anterior neuroectoderm specification during gastrulation. *Development* **121**, 3279-3290.

Acampora, D., Merlo, G. R., Paleari, L., Zerega, B., Postiglione, M. P., Mantero, S., Bober, E., Barbieri, O., Simeone, A. and Levi, G. (1999). Craniofacial, vestibular and bone defects in mice lacking the Distal-less-related gene Dlx5. *Development* **126**, 3795-3809.

Alvarez, Y., Alonso, M. T., Vendrell, V., Zelarayan, L. C., Chamero, P., Theil, T., Bosl, M. R., Kato, S., Maconochie, M., Riethmacher, D. et al. (2003). Requirements for FGF3 and FGF10 during inner ear formation. *Development* **130**, 6329-6338.

Anderson, D. W., Probst, F. J., Belyantseva, I. A., Fridell, R. A., Beyer, L., Martin, D. M., Wu, D., Kachar, B., Friedman, T. B., Raphael, Y. et al. (2000). The motor and tail regions of myosin XV are critical for normal structure and function of auditory and vestibular hair cells. *Hum. Mol. Genet.* **9**, 1729-1738.

Ang, S. L., Jin, O., Rhinn, M., Daigle, N., Stevenson, L. and Rossant, J. (1996). A targeted mouse Otx2 mutation leads to severe defects in gastrulation and formation of axial mesoderm and to deletion of rostral brain. *Development* **122**, 243-252.

Bok, J., Bronner-Fraser, M. and Wu, D. K. (2004). Role of hindbrain in dorsoventral but not anteroposterior axial specification of the inner ear. *Development* **132**, 2115-2124.

Bouillet, P., Chazaud, C., Oulad-Abdelghani, M., Dolle, P. and Chambon, P. (1995). Sequence and expression pattern of the Stra7 (Gbx-2) homeobox-containing gene induced by retinoic acid in P19 embryonal carcinoma cells. *Dev. Dyn.* **204**, 372-382.

Broccoli, V., Boncinelli, E. and Wurst, W. (1999). The caudal limit of Otx2 expression positions the isthmic organizer. *Nature* **401**, 164-168.

Burton, Q., Cole, L. K., Mulheisen, M., Chang, W. and Wu, D. K. (2004). The role of Pax2 in mouse inner ear development. *Dev. Biol.* **272**, 161-175.

Cantos, R., Cole, L. K., Acampora, D., Simeone, A. and Wu, D. K. (2000). Patterning of the mammalian cochlea. *Proc. Natl. Acad. Sci. USA* **97**, 11707-11713.

Chiang, C., Young, K. E. and Beachy, P. A. (1995). Control of Drosophila tracheal branching by the novel homeodomain gene unplugged, a regulatory target for genes of the bithorax complex. *Development* **121**, 3901-3912.

Cordes, S. P. and Barsh, G. S. (1994). The mouse segmentation gene kr encodes a novel basic domain-leucine zipper transcription factor. *Cell* **79**, 1025-1034.

Depew, M. J., Liu, J. K., Long, J. E., Presley, R., Meneses, J. J., Pedersen,

R. A. and Rubenstein, J. L. (1999). Dlx5 regulates regional development of the branchial arches and sensory capsules. *Development* **126**, 3831-3846.
Dottori, M., Hartley, L., Galea, M., Paxinos, G., Polizzotto, M., Kilpatrick, T., Bartlett, P. F., Murphy, M., Kontgen, F. and Boyd, A. W. (1998). EphA4 (Sek1) receptor tyrosine kinase is required for the development of the corticospinal tract. *Proc. Natl. Acad. Sci. USA* **95**, 13248-13253.
Dressler, G. R., Deutsch, U., Chowdhury, K., Nornes, H. O. and Gruss, P. (1990). Pax2, a new murine paired-box-containing gene and its expression in the developing excretory system. *Development* **109**, 787-795.
Everett, L. A., Belyantseva, I. A., Noben-Trauth, K., Cantos, R., Chen, A., Thakkar, S., Hoogstraten-Miller, S., Kachar, B., Wu, D. K. and Green, E. (2001). Targeted disruption of mouse Pds provides key insight about the inner-ear defects encountered in Pendred syndrome. *Hum. Mol. Genet.* **10**, 153-161.
Fekete, D. M. (1996). Cell fate specification in the inner ear. *Curr. Opin. Neurobiol.* **6**, 533-541.
Fekete, D. M. (1999). Development of the vertebrate ear: insights from knockouts and mutants. *Trends Neurosci.* **22**, 263-269.
Giudicelli, F., Gilardi-Hebenstreit, P., Mechta-Grigoriou, F., Poquet, C. and Charnay, P. (2003). Novel activities of Mafb underlie its dual role in hindbrain segmentation and regional specification. *Dev. Biol.* **253**, 150-162.
Hadrys, T., Braun, T., Rinkwitz-Brandt, S., Arnold, H. H. and Bober, E. (1998). Nkx5-1 controls semicircular canal formation in the mouse inner ear. *Development* **125**, 33-39.
Hidalgo-Sanchez, M., Alvarado-Mallart, R. and Alvarez, I. S. (2000). Pax2, Otx2, Gbx2 and Fgf8 expression in early otic vesicle development. *Mech. Dev.* **95**, 225-229.
Hulander, M., Kiernan, A. E., Blomqvist, S. R., Carlsson, P., Samuelsson, E. J., Johansson, B. R., Steel, K. P. and Enerback, S. (2003). Lack of pendrin expression leads to deafness and expansion of the endolymphatic compartment in inner ears of Foxi1 null mutant mice. *Development* **130**, 2013-2025.
Karis, A., Pata, I., van Doorninck, J. H., Grosveld, F., de Zeeuw, C. I., de Caprona, D. and Fritzsch, B. (2001). Transcription factor GATA-3 alters pathway selection of olivocochlear neurons and affects morphogenesis of the ear. *J. Comp. Neurol.* **429**, 615-630.
Kiernan, A. E., Nunes, F., Wu, D. K. and Fekete, D. M. (1997). The expression domain of two related homeobox genes defines a compartment in the chicken inner ear that may be involved in semicircular canal formation. *Dev. Biol.* **191**, 215-229.
Kiernan, A. E., Steel, K. P. and Fekete, D. M. (2002). Development of the Mouse Inner Ear. In *Mouse Development: Patterning, Morphogenesis, and Organogenesis*, Vol. 1 (ed. J. Rossant and P. P. L. Tam), pp. 539–566. Orlando, FL: Academic Press.
Ma, Q., Chen, Z., Barrantes, I., de la Pompa, J. L. and Anderson, D. J. (1998). Neurogenin 1 is essential for the determination of neuronal precursors for proximal cranial sensory ganglia. *Neuron* **20**, 469-482.
Mahmood, R., Mason, I. J. and Morriss-Kay, G. M. (1996). Expression of Fgf-3 in relation to hindbrain segmentation, otic pit position and pharyngeal arch morphology in normal and retinoic acid-exposed mouse embryos. *Anat. Embryol.* **194**, 13-22.
Mansour, S. L., Goddard, J. M. and Capecchi, M. R. (1993). Mice homozygous for a targeted disruption of the proto-oncogene int-2 have developmental defects in the tail and inner ear. *Development* **117**, 13-28.
Marin, F. and Charnay, P. (2000). Hindbrain patterning: FGFs regulate Krox20 and mafB/kr expression in the otic/preotic region. *Development* **127**, 4925-4935.
McKay, I. J., Lewis, J. and Lumsden, A. (1996). The role of FGF-3 in early inner ear development: an analysis in normal and kreisler mutant mice. *Dev. Biol.* **174**, 370-378.
Merlo, G. R., Paleari, L., Mantero, S., Zerega, B., Adamska, M., Rinkwitz, S., Bober, E. and Levi, G. (2002). The Dlx5 homeobox gene is essential for vestibular morphogenesis in the mouse embryo through a BMP4-mediated pathway. *Dev. Biol.* **248**, 157-169.
Millet, S., Campbell, K., Epstein, D. J., Losos, K., Harris, E. and Joyner, A. L. (1999). A role for Gbx2 in repression of Otx2 and positioning the mid/hindbrain organizer. *Nature* **401**, 161-164.
Morsli, H., Choo, D., Ryan, A., Johnson, R. and Wu, D. K. (1998). Development of the mouse inner ear and origin of its sensory organs. *J. Neurosci.* **18**, 3327-3335.
Morsli, H., Tuorto, F., Choo, D., Postiglione, M. P., Simeone, A. and Wu, D. K. (1999). Otx1 and Otx2 activities are required for the normal development of the mouse inner ear. *Development* **126**, 2335-2343.
Niederreither, K., Vermot, J., Schuhbaur, B., Chambon, P. and Dolle, P. (2000). Retinoic acid synthesis and hindbrain patterning in the mouse embryo. *Development* **127**, 75-85.
Pirvola, U., Spencer-Dene, B., Xing-Qun, L., Kettunen, P., Thesleff, I., Fritzsch, B., Dickson, C. and Ylikoski, J. (2000). Fgf/Fgfr-2 (IIIb) signaling is essential for inner ear morphogenesis. *J. Neurosci.* **20**, 6125-6134.
Rhinn, M., Dierich, A., Shawlot, W., Behringer, R. R., le Meur, M. and Ang, S. L. (1998). Sequential roles for Otx2 in visceral endoderm and neuroectoderm for forebrain and midbrain induction and specification. *Development* **125**, 845-856.
Riccomagno, M. M., Martinu, L., Mulheisen, M., Wu, D. K. and Epstein, D. J. (2002). Specification of the mammalian cochlea is dependent on Sonic hedgehog. *Genes Dev.* **16**, 2365-2378.
Rinkwitz-Brandt, S., Justus, M., Oldenettel, I., Arnold, H. H. and Bober, E. (1995). Distinct temporal expression of mouse Nkx-5.1 and Nkx-5.2 homeobox genes during brain and ear development. *Mech. Dev.* **52**, 371-381.
Rinkwitz-Brandt, S., Arnold, H. H. and Bober, E. (1996). Regionalized expression of Nkx5-1, Nkx5-2, Pax2 and sek genes during mouse inner ear development. *Hear. Res.* **99**, 129-138.
Sham, M. H., Vesque, C., Nonchev, S., Marshall, H., Frain, M., Gupta, R. D., Whiting, J., Wilkinson, D., Charnay, P. and Krumlauf, R. (1993). The zinc finger gene Krox20 regulates HoxB2 (Hox2.8) during hindbrain segmentation. *Cell* **72**, 183-196.
Shamim, H. and Mason, I. (1998). Expression of Gbx-2 during early development of the chick embryo. *Mech. Dev.* **76**, 157-159.
Su, Y. and Meng, A. (2002). The expression of gbx-2 during zebrafish embryogenesis. *Mech. Dev.* **113**, 107-110.
Swiatek, P. J. and Gridley, T. (1993). Perinatal lethality and defects in hindbrain development in mice homozygous for a targeted mutation of the zinc finger gene Krox20. *Genes Dev.* **7**, 2071-2084.
Theil, T., Frain, M., Gilardi-Hebenstreit, P., Flenniken, A., Charnay, P. and Wilkinson, D. G. (1998). Segmental expression of the EphA4 (Sek-1) receptor tyrosine kinase in the hindbrain is under direct transcriptional control of Krox-20. *Development* **125**, 443-452.
Theil, T., Ariza-McNaughton, L., Manzanares, M., Brodie, J., Krumlauf, R. and Wilkinson, D. G. (2002). Requirement for downregulation of kreisler during late patterning of the hindbrain. *Development* **129**, 1477-1485.
Torres, M., Gomez-Pardo, E. and Gruss, P. (1996). Pax2 contributes to inner ear patterning and optic nerve trajectory. *Development* **122**, 3381-3391.
Vendrell, V., Carnicero, E., Giraldez, F., Alonso, M. T. and Schimmang, T. (2000). Induction of inner ear fate by FGF3. *Development* **127**, 2011-2019.
von Bubnoff, A., Schmidt, J. E. and Kimelman, D. (1996). The Xenopus laevis homeobox gene Xgbx-2 is an early marker of anteroposterior patterning in the ectoderm. *Mech. Dev.* **54**, 149-160.
Wang, W., van de Water, T. and Lufkin, T. (1998). Inner ear and maternal reproductive defects in mice lacking the Hmx3 homeobox gene. *Development* **125**, 621-634.
Wassarman, K. M., Lewandoski, M., Campbell, K., Joyner, A. L., Rubenstein, J. L., Martinez, S. and Martin, G. R. (1997). Specification of the anterior hindbrain and establishment of a normal mid/hindbrain organizer is dependent on Gbx2 gene function. *Development* **124**, 2923-2934.
Wright, T. J. and Mansour, S. L. (2003). Fgf3 and Fgf10 are required for mouse otic placode induction. *Development* **130**, 3379-3390.
Xu, P. X., Woo, I., Her, H., Beier, D. R. and Maas, R. L. (1997). Mouse Eya homologues of the Drosophila eyes absent gene require Pax6 for expression in lens and nasal placode. *Development* **124**, 219-231.
Xu, P. X., Adams, J., Peters, H., Brown, M. C., Heaney, S. and Maas, R. (1999). Eya1-deficient mice lack ears and kidneys and show abnormal apoptosis of organ primordia. *Nat. Genet.* **23**, 113-117.